A Wideband Transmitarray Using Dual-Resonant Double Square Rings

Colan G. M. Ryan, *Student Member, IEEE*, Mohammad Reza Chaharmir, *Member, IEEE*, J. Shaker, *Member, IEEE*, Joey R. Bray, *Member, IEEE*, Yahia M. M. Antar, *Fellow, IEEE*, and A. Ittipiboon, *Senior Member, IEEE*

***Abstract*—A four-layer transmitarray operating at 30 GHz is designed using a dual-resonant double square ring as the unit cell element. The two resonances of the double ring are used to increase the per-layer phase variation while maintaining a wide transmission magnitude bandwidth of the unit cell. The design procedure for both the single-layer unit cell and the cascaded connection of four layers is described and it leads to a 50% increase in the −1 dB gain bandwidth over that of previous transmitarrays. Results of a 7.5% −1 dB gain bandwidth and 47% radiation efficiency are reported.**

***Index Terms*—Broadband, double square ring, transmitarray.**

I. Introduction

ANTENNAS for satellite-based telecommunication systems should be high-gain, broadband, light-weight, and inexpensive to manufacture. Among the possible options, the transmitarray antenna is a promising potential technology to meet these requirements. It is simple to fabricate and its spatial feeding method does not suffer the insertion loss of a phased array's feed network at millimeter wave frequencies [1]. Comprised of a planar array of printed patch elements, the transmitarray avoids the fabrication complexity inherent in parabolic reflectors, and being usually less than one wavelength thick, it has size and weight advantages over shaped dielectric lenses. Furthermore, the feed can be placed directly in front of the aperture without incurring the blockage losses of a reflectarray configuration. The main drawback of the transmitarray is its limited bandwidth, which is usually around 5% or less. To overcome this bandwidth limitation while minimizing antenna thickness, this paper presents a novel transmitarray operating at 30 GHz which uses a double square ring as the unit cell element and offers a wider bandwidth than previously achieved.

To date, transmitarrays have been manufactured using stub-loaded patches or using elements connected through multiple layers by a delay line [2], [3]; however, these long lengths of line can make element placement difficult and can result in spurious cross-polarized radiation [1] or unwanted modes in the layered transmitarray [4]. Other authors have proposed the use of amplifier and phase-shifter stages to boost power levels in spatial power combiners or to create reconfigurable antennas [5], but this approach would increase both the cost and the complexity and would make the antenna's performance susceptible to failure of the active devices. In a method that simplifies the antenna fabrication, a third scheme has been implemented by Chaharmir *et al.* [6] in which four layers are cascaded and the phase change is accomplished by varying the length of the cross-dipole unit cell element. Although the use of multiple layers increases the antenna's thickness, weight and manufacturing cost, the smaller phase change required per layer can result in a larger bandwidth. Mindful of these tradeoffs, this paper will focus on increasing the bandwidth of a passive transmitarray operating at 30 GHz while employing the fewest number of layers required to achieve the necessary phase change.

In Section II, the operation of a transmitarray antenna is described and the rationale behind using the double square ring element is presented. Section III shows the simulation and optimization both of the double square ring element and of the multilayer transmitarray antenna. Measured radiation patterns yielding the antenna's gain and bandwidth are given in Section IV. Finally, the conclusions are drawn in Section V.

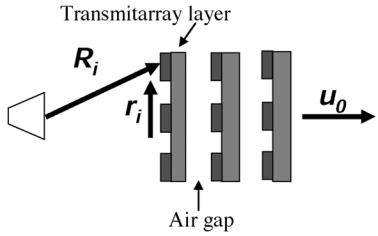

Fig. 1. Transmitarray geometry.

II. Background Theory

A. Transmitarray Operation

To collimate the incident wave from the feed horn, a transmitarray uses the antenna elements on its surface to re-phase the incoming spherical wave and then re-transmit the signal as a plane wave. The amount of phase adjustment needed at each antenna element depends on the phase delay an incident ray has accumulated travelling between the feed horn and the transmitarray surface. Fig. 1 denotes $\boldsymbol{R_i}$ as the vector to the ith element from the feed's phase centre, and $\boldsymbol{r_i}$ as the position vector to the ith element from the transmitarray centre; k is the propagation constant, and $\boldsymbol{u_0}$ is the direction of the transmitted main beam.

Manuscript received August 18, 2009; revised November 20, 2009; accepted November 26, 2009. Date of publication March 01, 2010; date of current version May 05, 2010.

C. G. M. Ryan was with the Royal Military College of Canada, Kingston, ON K7K 7B4, Canada. He is now with the Edward S. Rogers Sr. Department of Electrical and Computer Engineering, University of Toronto, Toronto, ON M5S 3G4, Canada (e-mail: colan.ryan@utoronto.ca).

M. R. Chaharmir, J. Shaker, and A. Ittipiboon are with the Communications Research Centre, Ottawa, ON K2H 8S2, Canada.

Y. M. M. Antar and J. R. Bray are with the Department of Electrical and Computer Engineering, Royal Military College, Kingston, ON K7K 7B4, Canada.

Digital Object Identifier 10.1109/TAP.2010.2044356

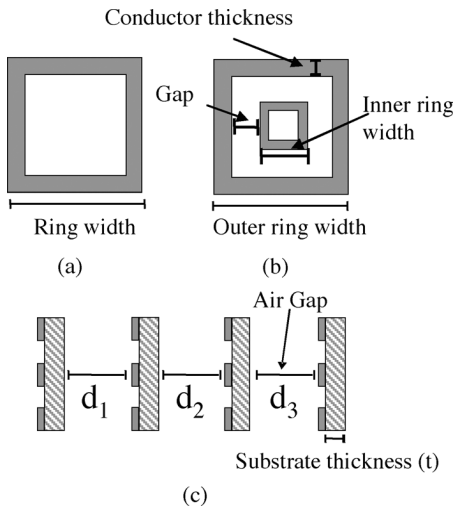

Fig. 2. (a) Single square ring element (b) double square ring element and (c) arrangement on multilayer transmitarray.

From [6], the necessary phase compensation value Φ_{i} at each element is given by (1):

$$\Phi_{\mathrm{i}} + k[\boldsymbol{R_i} + \boldsymbol{r_i} \cdot \boldsymbol{u_0}] = 2\pi n,\ n = 0, 1, 2, \ldots. \qquad (1)$$

The antenna should theoretically be capable of producing a transmission phase shift of between 0° and 360° at each element location; as will be seen, however, good performance can be achieved even with a slightly smaller phase range. In the proposed design, the desired phase shift from each element is obtained by changing the element's dimensions around its resonant size. The impedance seen by the incident wave changes with the cell geometry and so the required phase compensation value can be specified.

The transmitarray must also possess a sufficient transmission magnitude to allow the incident signal to pass through the antenna; blocking ray transmission even at certain points leads to phase errors and decreased gain, thus nullifying the advantage of proper phase compensation. Therefore, the design process must involve both the elements' transmission phase shift and magnitude.

B. The Double Square Ring Element

The first goal of this work is to increase the transmitarray bandwidth, which is primarily limited by the bandwidth of the element itself [5]. A square loop element as shown in Fig. 2(a) has been chosen to address this issue since it has already been demonstrated to have wide bandwidth performance in reflectarray antennas [7]. Furthermore, the small resonant size enables close element packing which improves the stability of the angular response [8]. Finally, as shown in [9], the fundamental mode current distribution excited by a normally incident linearly polarized wave is primarily concentrated on the ring arms parallel to the incident field's polarization. Consequently, the re-transmitted wave should also be linearly polarized and as currents on the horizontal ring sections are oppositely directed, low cross-polarization is expected from this element.

To reduce the number of layers that are required in the transmitarray antenna, the per-layer phase change should be maximized. For this reason, a second concentric ring has been added to yield the double square ring element, as shown in Fig. 2(b). The transmission magnitude and phase versus frequency graphs are illustrated for generic single- and double-square ring geometries in Fig. 3. As the dimensions of the element change, the magnitude and phase responses shift higher or lower in frequency, and thus the phase change seen at a particular frequency can be controlled.

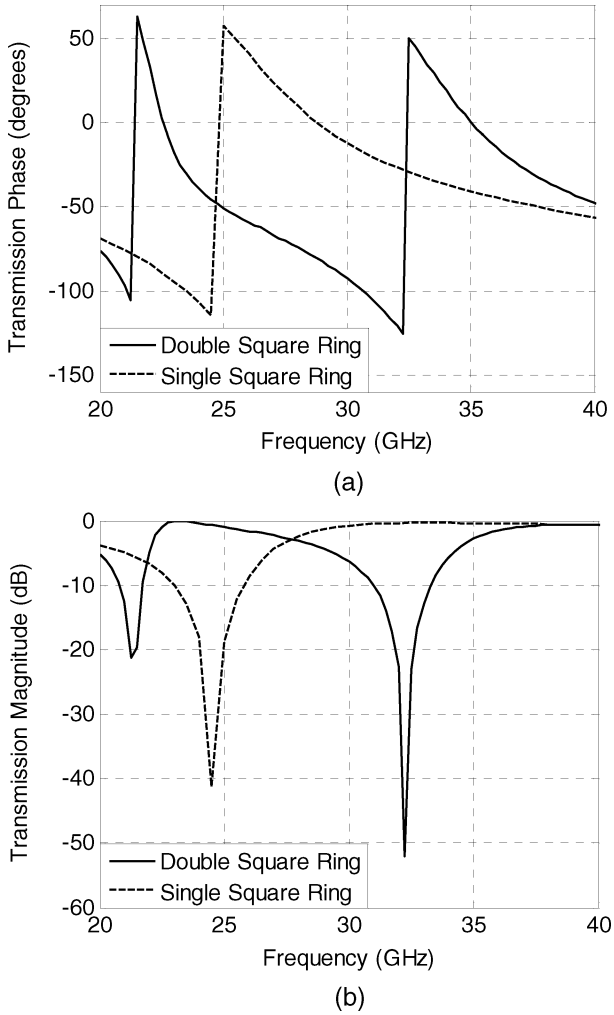

Fig. 3. Illustration of (a) phase response and (b) magnitude response for generic single- and double-square ring elements.

In optimizing the position of the two resonances, the extra degree of freedom of the inner ring can be used to find the best balance between the phase change and the transmission magnitude bandwidth. From Fig. 3, it is seen that the addition of the second inner ring has introduced a second resonance in the frequency response and has increased the slope of the phase-versus- frequency curve between the two resonances. At a cost of a reduced transmission magnitude bandwidth (i.e., good transmission is obtained between the two resonances at 22 GHz and 32.5 GHz) a greater total phase change can be obtained from the double square ring element as its dimensions are varied. This increased per-layer phase change results in fewer layers necessary to achieve the full 360° coverage and the antenna's thickness, weight, cost, and fabrication complexity correspondingly

decrease. Consequently, the challenge in using such a dual-resonant element is to exploit the rapidly-varying frequency response to increase the phase change while simultaneously maximizing the transmission magnitude across the desired operating band.

III. Design of the Unit Cell Element

A. Four Possible Unit Cells

To optimize both the transmission magnitude and phase responses of the double-square ring element, HFSS was used to simulate the unit cell element of this transmitarray antenna [10]. To account for coupling between elements, perfect electric- and magnetic-wall boundary conditions were imposed around the unit cell to simulate an infinite layer of elements. In each simulation, lossless materials were assumed and only normal incidence angles were considered for a linearly polarized incident wave.

Four different design strategies were investigated and are illustrated in Fig. 4. In the "fixed-gap" approach, the gap size between the inner and outer rings was set to a constant value and the width of the element was varied in order to control the phase variation. In an effort to improve the bandwidth, the second strategy employed a "variable-gap," in which the gap size is a function of the element width; this approach was used to delay the onset of the second resonance into the desired 30 GHz operating band. A "double-sided" design was also investigated to determine if an increased coupling between the rings could either widen the element bandwidth or lead to a larger per-layer phase change. Finally, an element with a fixed outer ring width was simulated; in this case the phase variation is controlled by specifying the width of the inner ring. This last design is unique in that it combines two different geometries which together are meant to cover the full 360° phase range. These two geometries differ in the width of their outer rings, but both implement the phase compensation by varying the width of their respective inner rings. Covering different, non-overlapping phase ranges, both geometries are to be used on each transmitarray layer depending upon what phase compensation value is required.

The following sub-section describes the design sequence of the "fixed-outer-ring" element, although similar optimization procedures were performed for each of the four unit cell elements shown in Fig. 4.

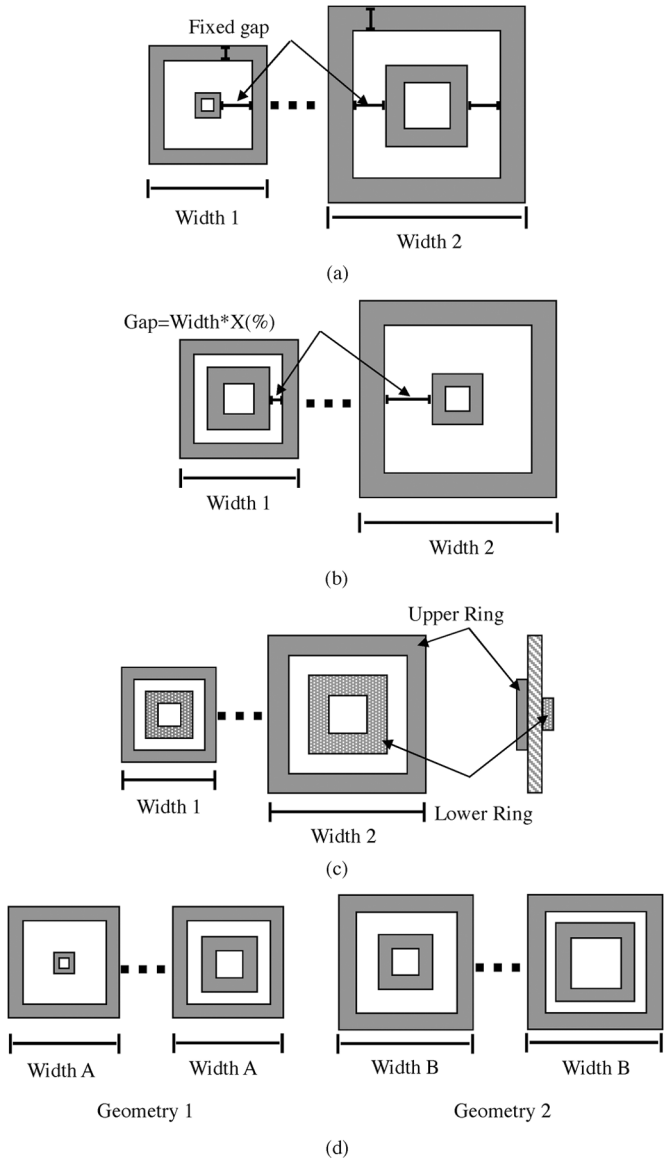

Fig. 4. Possible unit cell designs: (a) fixed-gap, (b) variable-gap, (c) double-sided, and (d) fixed-outer ring.

B. Single Layer Design for Fixed-Outer Ring Unit Cell

In this design, the transmission phase shift is controlled by varying the width of the inner ring while the outer ring width is fixed. This approach has an important advantage over a design in which the widths of both rings are varied simultaneously: fixing one resonant frequency yields a larger transmission magnitude bandwidth than can be obtained by trying to vary both frequencies simultaneously.

The cell size and substrate type are common to both geometries used for this unit cell and were consequently the first parameters to be optimized. A square lattice with a cell size of 6 mm was selected to preclude grating lobe formation for feed incidence angles of up to 30°, corresponding to the maximum angle of incidence experienced for the intended focal length-to-diameter (F/D) ratio of 0.9. The substrate's relative permittivity of $\varepsilon_{\mathrm{r}} = 2.2$ was selected to centre the element's resonant frequencies around the 30 GHz operating band. The thickness of the substrate was also optimized. Fig. 5 plots the transmission magnitude and phase versus frequency for a double square ring element for several different substrate thicknesses. The higher-frequency resonances (corresponding to the smaller ring) show a greater frequency sensitivity to variations in the substrate height than do those of the wider ring. The results show that as the substrate thickness increases, the separation between inner and outer ring resonant frequencies decreases, thus reducing the element's transmission magnitude bandwidth.

The element on the thickest substrate produces the most rapid rate of transmission phase and magnitude variation with frequency. Therefore, at a given frequency, the large phase change which can be implemented by each layer could result in fewer overall layers required in the transmitarray. However, a consequence of the accompanying rapid magnitude variation is that

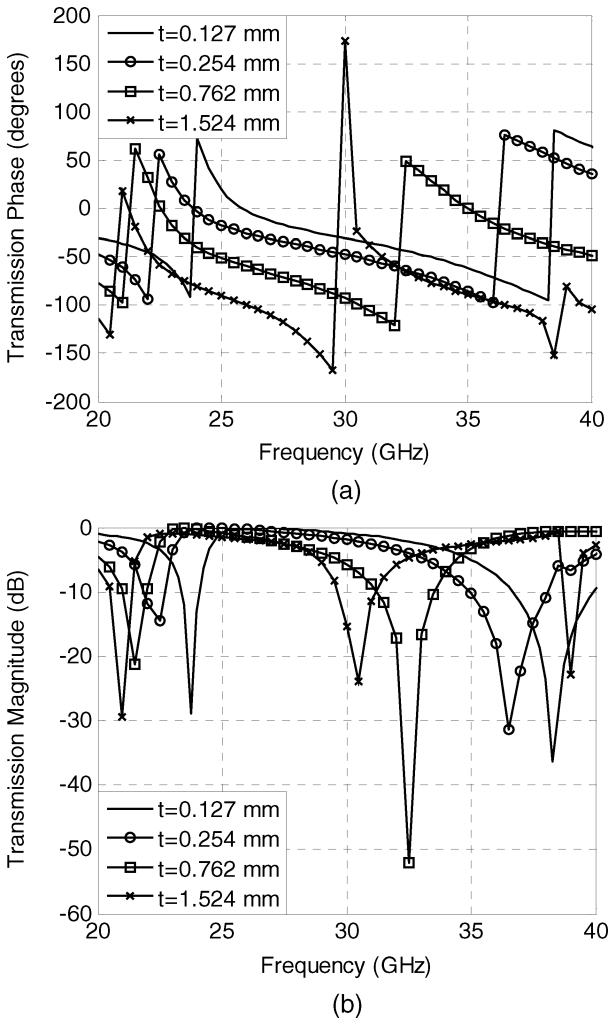

Fig. 5. Transmission phase (a) and magnitude (b) versus frequency for several substrate thicknesses (t). Double square ring element dimensions: inner and outer ring thickness $= 0.2$ mm, outer ring width $= 3$ mm, inner ring width $= 2.2$ mm, $\varepsilon_r = 2.2$, cell size $= 6$ mm.

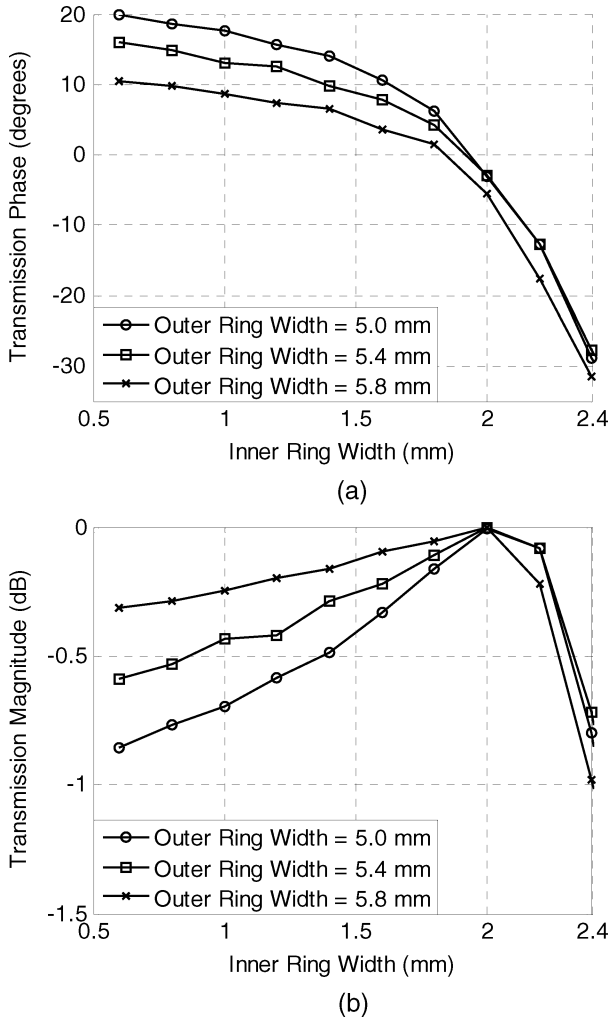

Fig. 6. Transmission phase (a) and magnitude (b) versus inner ring width for several different outer ring widths at 30 GHz.

even a small change in the element's dimensions could degrade the transmission magnitude, thus nullifying the intended phase compensation as described previously. To increase the transmitarray bandwidth, more gradual phase and magnitude variations are desired and therefore, the thinnest substrate of thickness 0.127 mm is chosen as the best option. This choice was also applied to each of the other three possible unit cell configurations.

To find the optimum dimensions for the "fixed-outer-ring" element, the size of the outer ring is varied to investigate its effect on the achievable phase change of the unit cell. To allow for a large variation in inner ring width, the conductor thickness of the inner ring is set to our minimum practical dimension of 0.2 mm, and the outer ring's conductor thickness is also initially set to this same value. Fig. 6 shows the single-layer 30 GHz transmission magnitude and phase responses versus inner ring width for several different outer ring widths. The results show that as the size of the outer ring is reduced, the transmission per-layer phase change increases from 41° up to 50°, but the transmission magnitude decreases at both the smallest and largest inner ring widths. With the twin goals of wide bandwidth and minimum transmitarray antenna thickness in mind, the outer ring width of 5.4 mm is selected as the best compromise between transmission magnitude bandwidth and phase change. Since a parametric study of both the inner and outer ring conductor thicknesses yielded no appreciable improvements over the current design, the dimensions of Geometry 1 for the fixed-outer ring unit cell were set according to Table I.

The dimensions of Geometry 2 were chosen such that both inner and outer ring resonances occur below the operating frequency of 30 GHz; this choice reduces the rate of phase variation as well as the per-layer phase change achievable by Geometry 2, but ensures high transmission magnitude over the operating frequency. To lower its resonant frequency, the inner ring size for Geometry 2 must be increased, and a larger outer ring width is in turn used to allow for a greater variation of inner ring size. The final dimensions of both geometries are specified in Table I.

As mentioned earlier, a similar design process was followed for each of the three remaining unit cell geometries. The optimized dimensions for each approach are given in Table I, and the single-layer transmission magnitude and phase responses for each of the four design strategies are compared in Fig. 7. Of these four unit cell designs, the fixed-gap and variable-gap

TABLE I
DIMENSIONS OF UNIT CELL CONFIGURATIONS AND OF TRANSMITARRAY ANTENNA

	Fixed Gap	Variable Gap	Double Sided	Fixed Outer Ring	
Parameter				Geometry 1	Geometry 2
Conductor Width	0.2 mm	0.2 mm (outer), 0.2 mm (inner)	0.2 mm (upper), 0.9 mm (lower)	0.2 mm	0.2 mm
Gap	1.3 mm	0.2mm+(W-2mm)•Rate	0.4 mm	NA	NA
Inner Ring Width	N/A	N/A	N/A	0.6-2.4 mm	4.2-5.0 mm
Outer Ring Width	4.0-5.4 mm	3.2-5.4 mm	2.6-3.8 mm	5.4 mm	5.8 mm
Cell Size	6.0 mm	6.0 mm	6.0 mm	6.0 mm	6.0 mm
Substrate Thickness (t)	0.127 mm	0.127 mm	0.127 mm	0.127 mm	0.127 mm
Relative Permittivity	3	3	2.2	2.2	2.2
Transmitarray Dimensions	(Not constructed)	(Not constructed)	(Not constructed)	12.6 cm x 12.6 cm	
Layer Separation				d_1=3 mm, d_2=3 mm, d_3=3 mm	

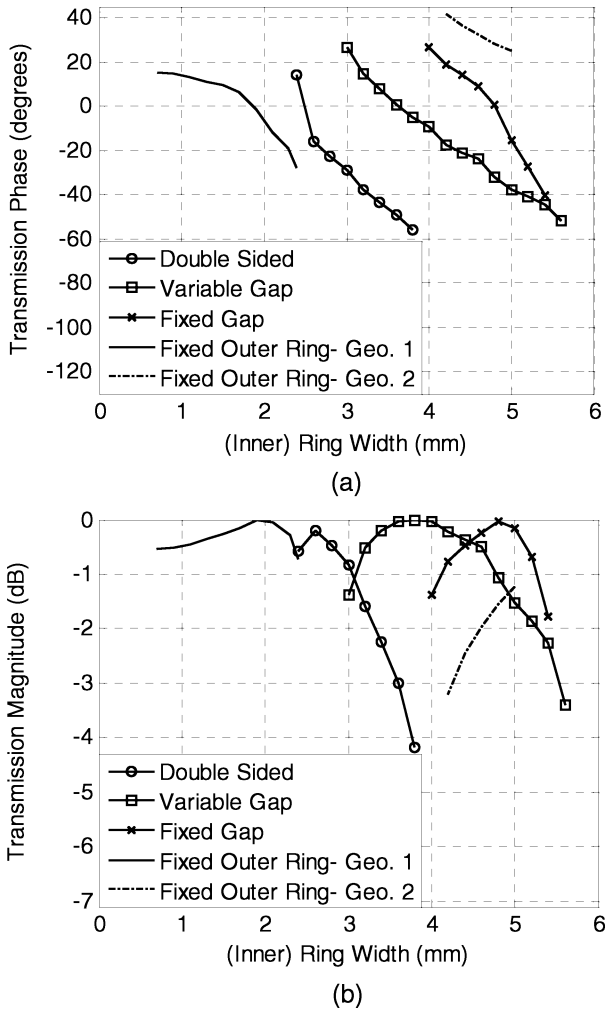

Fig. 7. Comparison of single layer phase (a) and magnitude (b) responses versus ring width/inner ring width, as applicable.

shows the largest phase variation (approximately 80°) as a function of the ring width. However, the transmission magnitude of the fixed-gap option drops rapidly as its width is varied around its resonant dimension; the same is true for the double-sided design. Such behavior implies a small element transmission bandwidth which will consequently limit the bandwidth of a multilayer antenna based on these two structures. The variable-gap approach is an appealing option due to its large phase variation and relatively slowly varying magnitude response. However, precise fabrication control is necessary to implement this choice since the gap dimension is calculated as a percentage of the overall element width. Therefore, it was deemed to be infeasible for the present application. Over its two geometries, the fixed-outer-ring unit cell produces approximately 70° of phase variation with a transmission magnitude that is either equal to or better than that of the competing designs. Furthermore, applying its two different geometries results in a larger number of phase points that can be applied to compensate the incoming wave, thus decreasing the quantization error of the phase response. As was shown in an earlier work, smaller phase errors of the fixed-outer ring unit cell lead to a higher antenna gain [11]. Therefore, the fixed-outer-ring element was chosen for the transmitarray unit cell.

C. Multilayer Design

Having selected the fixed-outer-ring approach and having determined the optimized single-layer dimensions for this unit cell, the next step is to simulate the multilayer structure. To avoid time-consuming full-wave simulations, the matrix propagator method of [12] was used to calculate the frequency response of the proposed design for two-, three-, and four-layer structures for a variety of layer separations from 1 mm up to 10 mm. The use of this matrix propagator approach can be justified by noting that the separation between layers is large enough to avoid significant near field coupling, and consequently, good agreement between the matrix propagator technique and a full-wave simulation is expected. An identical 3 mm air gap between each of the layers was found to yield the highest 30 GHz transmission magnitude over the intended inner ring width range for all three multilayer designs. The multilayer structures for this optimum layer spacing were then simulated in HFSS and Fig. 8 shows the 30 GHz transmission magnitude and phase curves versus inner ring width for different multilayer geometries; in each case, the separation between layers is 3 mm. The four-layer magnitude and phase responses calculated from the matrix propagator method are superimposed on the graphs; good agreement between the two approaches is obtained. Note that the graphs also indicate the range of values covered by each of the two geometries. The

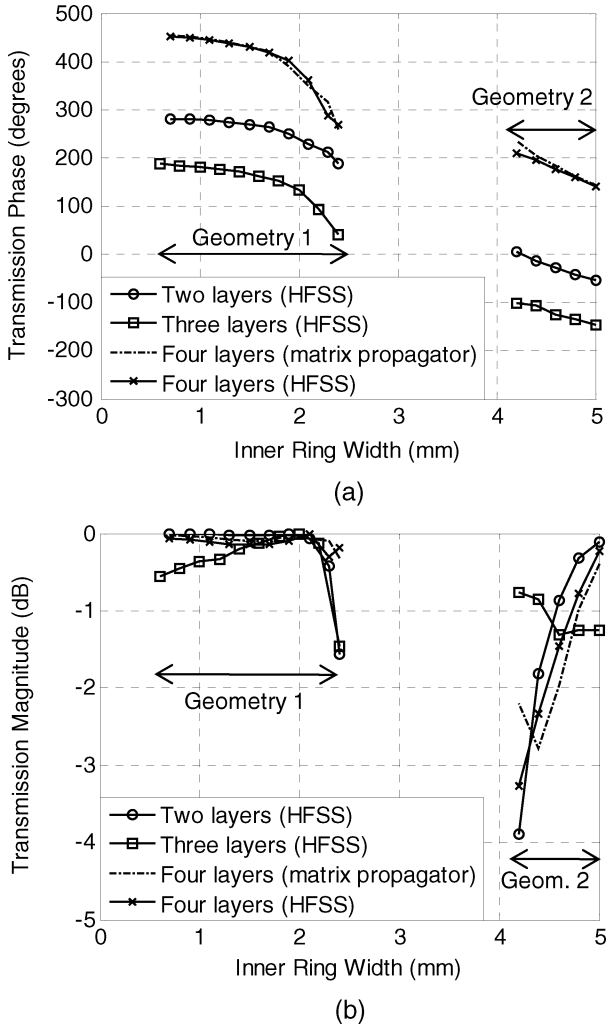

Fig. 8. Comparison at 30 GHz of multilayer transmission phase (a) and magnitude (b) versus inner ring width for two, three, and four cascaded identical layers with a 3 mm layer separation.

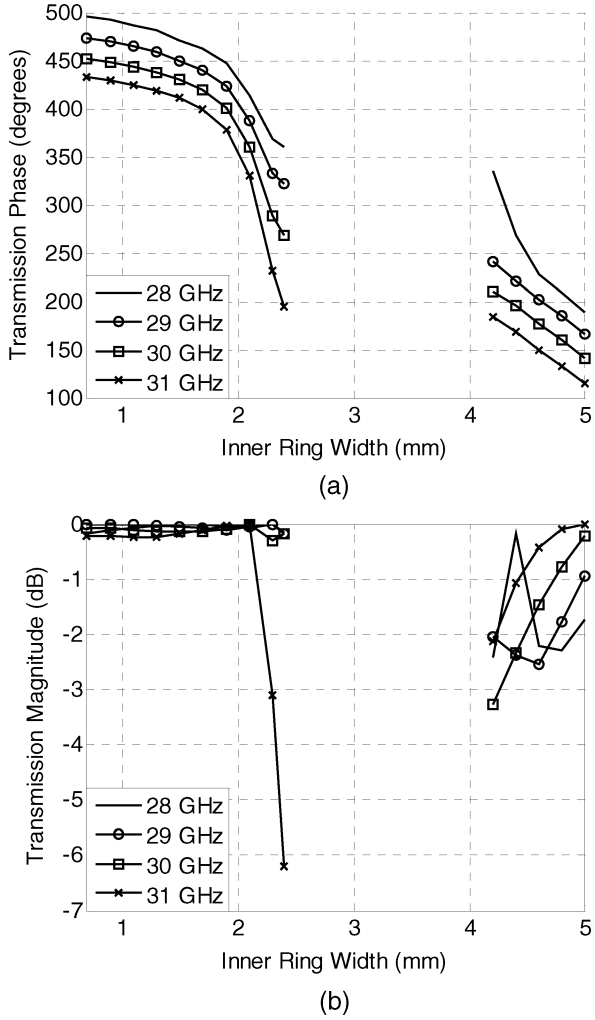

Fig. 9. Transmission phase (a) and magnitude (b) versus inner ring width for a four-layer structure for several different frequencies.

results show that the minimum transmission magnitude experienced by the configurations is -4 dB. The figure also shows the two geometries of the four-layer design cover approximately 270° in total. Reducing the number of layers decreases the range of phase compensation values and will lead to phase errors in the transmitted wavefront. Therefore, the four-layer design is selected as the best option.

Fig. 9 plots the transmission magnitude and phase responses versus inner ring width for a four-layer structure for several frequencies ranging from 28 GHz to 31 GHz. A minimum of 270° phase variation is achieved at each frequency across the band and the transmission magnitude over the width range is usually above -3 dB. The transmission magnitude begins to decrease for frequencies above 31 GHz.

IV. Measured Results and Discussion

The four-layer transmitarray with the fixed-outer-ring unit cell was fabricated according to the dimensions of Table I with an F/D ratio of 0.9. A Rogers RT/Duroid 5880 substrate was used and foam spacers were inserted between the layers to create the air gaps. Fig. 10 shows the measured far-field H-plane and E-plane radiation patterns at 30 GHz as well as the measured peak H-plane gain versus frequency.

Using the multilayer transmission magnitude and phase properties simulated in HFSS, array theory is used to calculate the radiation patterns of this transmitarray at 30 GHz and these results are superimposed upon the measured data in Fig. 10. The directivity of an ideal aperture (i.e., that with perfect phase compensation and unity transmission magnitude) at 30 GHz of equal dimensions to the current antenna and with the feed pattern modeled by a $\cos^9(\theta)$ distribution is calculated to be 31.9 dB; consequently, the measured H- and E-plane gains at 30 GHz of 28 dB and 28.14 dB correspond to radiation efficiencies of 41% and 42%, respectively. Corresponding to a peak efficiency of 47%, the measured peak gain of 28.59 dB occurs slightly off the center frequency at 30.25 GHz.

The first sidelobe levels in the H- and E-planes are approximately -16.5 dB and -19.5 dB below the main peaks, respectively. This difference is likely due to the asymmetry in the rectangular horn feed pattern resulting in different aperture illuminations in the two planes. To the authors' knowledge the -1 dB gain bandwidth of 2.25 GHz (7.5%) is the largest bandwidth

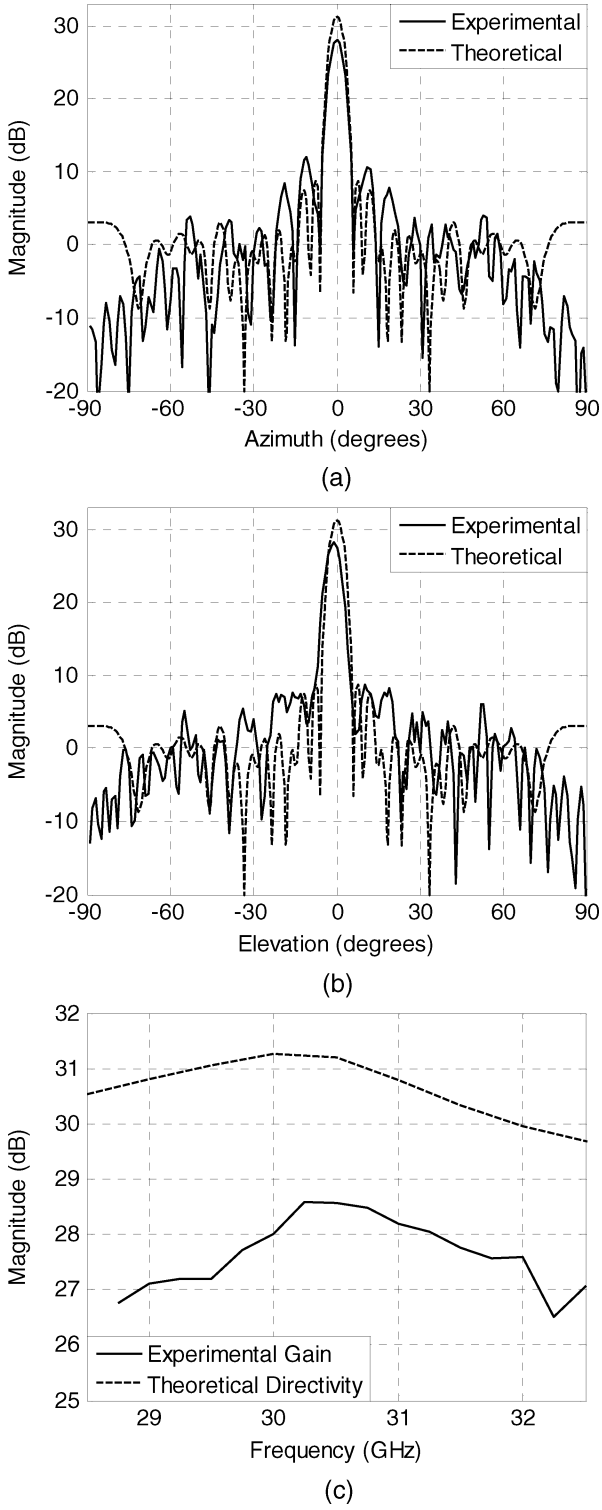

Fig. 10. Measured and simulated 30 GHz radiation pattern for (a) H-plane, (b) E-plane, and (c) H-plane gain versus frequency.

that has yet been achieved by a transmitarray antenna. The measured results are compared against the simulated performance in Table II.

Discrepancies between the measured and simulated results can be attributed to a variety of factors. Neglecting dielectric and conductor losses likely contributed to the slightly smaller-than-expected radiation efficiency; simulated per-layer loss is approximately 0.25 dB, while the loss due to each of the three foam spacer was measured to be nearly 0.3 dB. Furthermore, assuming that the feed signal is normally incident on all of the elements leads to errors in the magnitude and phase response of elements which are actually illuminated by oblique incidence angles; these errors cause a decrease in antenna gain. For instance, additional simulations for incidence angles of up to 30° indicate the per-layer transmission magnitude may decrease by up to 1.3 dB over the normal incidence case. The errors between measured and simulated results at grazing angles may result from two different sources. First, the infinite array assumption inherent in the boundary conditions applied in HFSS does not represent a finite-sized transmitarray layer, and so the frequency response of the edge elements in particular will differ from the simulated values. Secondly, feed signal diffraction from the antenna edges is not accounted for in the calculated pattern. A final source of error is in the manufacturing tolerances of ± 0.1 mm which could have resulted in additional phase errors in the wavefront compensation. Taking these errors together, and considering that multiple layers are used in the antenna, a peak radiation efficiency of 47% is reasonable and is well within the typical range for transmitarrays. Therefore, the combination of relatively high efficiency, a -1 dB gain bandwidth of 7.5%, and simple construction techniques show the potential of double-resonant elements in transmitarray antennas.

TABLE II
COMPARISON OF TRANSMITARRAY MEASURED AND SIMULATED PERFORMANCE

Parameter	Measured Value	Theoretical Value
Peak gain	28.59 dB	31.26 dB
Peak radiation efficiency	47% at 30.25 GHz	85% at 30 GHz
Sidelobe level (H-plane, E-plane)	–16.5dB, –19.5 dB	–23 dB
–1 dB gain bandwidth	2.25 GHz (7.5%)	3.25 GHz (10.8%)

V. CONCLUSION

This work has demonstrated the design of a novel transmitarray antenna using dual-resonant double square ring elements. A new approach has been proposed in which varying the elements' inner ring widths specifies the phase of the transmitted wave and in which a second element geometry is incorporated to increase the total achievable phase range for wavefront compensation. The additional degree of freedom of the inner rings' resonances has been used to improve the antenna's -1 dB gain bandwidth over previous designs without sacrificing other performance metrics.

REFERENCES

[1] J. Huang and J. A. Encinar, *Reflectarray Antennas*. Hoboken, NJ: Wiley, 2008.

[2] K.-W. Lam, S.-W. Kwok, Y. Hwang, and T. Lo, "Implementation of transmitarray antenna concept by using aperture coupled microstrip patches," in *Proc. Asia-Pacific Microwave Conf.*, Hong Kong, 1997, vol. 1, pp. 433–436.

[3] H. Sun and W. Zhang, "Design of broadband element of transmitarray with polarization transform," in *Int. Workshop on Antenna Technology: Small and Smart Antennas, Metamaterials and Applications*, Cambridge, U.K., 2007, pp. 287–290.

[4] P. de la Torre, M. Sierra-Castañer, and M. Sierra-Pérez, "Design of a double array lens," in *1st Eur. Conf. on Antennas and Propagation*, Nice, France, 2006, pp. 1–5.
[5] F.-C. E. Tsai and M. E. Bialkowski, "Investigations into the design of a spatial power combiner employing a planar transmitarray of stacked patch antennas," in *Proc. 15th Int. Conf. on Microwaves, Radar and Wireless Communications*, May 17–19, 2004, vol. 2, pp. 509–512.
[6] M. R. Chaharmir, A. Ittipiboon, and J. Shaker, "Single-band and dual-band transmitarray," presented at the 10th Int. Symp. on Antenna Technology and Applied Electromagnetics, Montreal, QC, 2006.
[7] M. R. Chaharmir, J. Shaker, M. Cuhaci, and A. Ittipiboon, "A broadband reflectarray antenna with double square rings as the cell elements," *Microwa. Opt. Technol. Lett.*, vol. 48, no. 7, pp. 317–1319, July 2006.
[8] B. Munk, *Frequency Selective Surfaces: Theory and Design*. New York: Wiley, 2000.
[9] S. M. A. Hamdy and E. A. Parker, "Current distribution on the elements of a square loop frequency selective surface," *IET Electron. Lett.*, vol. 18, no. 14, pp. 624–626, Jul. 1982.
[10] [Online]. Available: http://www.ansoft.comAnsoft HFSS, The 3D, electromagnetic, finite-element simulation tools for high-frequency design
[11] C. G. M. Ryan, M. R. Chaharmir, J. Shaker, J. R. Bray, Y. M. M. Antar, and A. Ittipiboon, "A broadband transmitarray using double square ring elements," presented at the 13th Int. Symp. on Antenna Technology and Applied Electromagnetics, Banff, AB, 2009.
[12] T. Cwik and R. Mittra, "The cascade connection of planar periodic surfaces and lossy dielectric layers to form an arbitrary periodic screen," *IEEE Trans. Antennas Propag.*, vol. 35, no. 12, pp. 1397–1405, Dec. 1987.

Colan G. M. Ryan (S'03) received the B.A.Sc. degree in electrical engineering from the University of Ottawa, in Ottawa, ON, Canada, in 2007 and the M.A.Sc. degree in electrical engineering from the Royal Military College of Canada, in Kingston, ON, Canada, in 2009.

In 2005, he held a co-op position with Edgewater Computer Systems. In 2006, he held a summer position as an NSERC Undergraduate Student Researcher in the Department of Electronics at Carleton University in Ottawa, Canada, where he developed a reconfigurable PIFA antenna for wireless mobile devices. He is currently working towards the Ph.D. degree in electrical engineering from the University of Toronto, Toronto, ON, Canada. His main research interests are antennas, periodic structures, and transmission-line metamaterials.

Mohammad Reza Chaharmir (M'04) received the B.Sc. degree (with honors) in electrical engineering from K.N. Toosi University of Technology, Tehran, Iran, in 1993, the M.Sc. degree in electrical engineering from Amir Kabir University of Technology, Tehran, in 1996, and Ph.D. degree from the University of Manitoba, Canada, in 2004.

He joined Communication Research Centre (CRC), Ottawa, ON, Canada, in 2001 as a microwave and antenna Engineer and was promoted to Research Scientist in 2005. He has also been an Adjunct Professor at Concordia University, Montreal, Canada, since 2005. His research interests and activities include periodic structures, reflectarray antennas, FSS, photonic bandgaps, metamaterials and antenna beam scanning.

J. Shaker is with the Communication Research Centre (CRC), Ottawa, ON, Canada.

Joey R. Bray (S'96–M'04) received the B.A.Sc. and M.A.Sc. degrees in electrical engineering from the University of Ottawa, Ottawa, ON, Canada, in 1995 and 1998, respectively, and the Ph.D. degree in electrical engineering from Carleton University, Ottawa, ON, Canada, in 2003.

In 2003, he joined the Department of Electrical and Computer Engineering at the Royal Military College of Canada, Kingston, ON, Canada, where he is currently an Associate Professor. From 2001 to 2002, he was a Visiting Researcher at Valtion Teknillinen Tutkimuskeskus (VTT) Electronics, Oulu, Finland. His research interests include ferrite microwave devices and microwave passive devices.

Dr. Bray received the Young Scientist Award in 2005 from the International Union of Radio Science (URSI).

Yahia M. M. Antar (S'73–M'76–SM'85–F'00) received the B.Sc. (Hons.) degree from Alexandria University, in 1966, and the M.Sc. and Ph.D. degrees from the University of Manitoba, in 1971 and 1975, respectively, all in electrical engineering.

In May 1979, he joined the Division of Electrical Engineering, National Research Council of Canada, Ottawa, where he worked on polarization radar applications in remote sensing of precipitation, radio wave propagation, electromagnetic scattering and radar cross section investigations. In November 1987, he joined the staff of the Department of Electrical and Computer Engineering at the Royal Military College of Canada in Kingston, where he has held the position of professor since 1990. He has authored or coauthored over 160 journal papers and 300 Conference papers, and holds several patents.

Dr. Antar is a Fellow of the IEEE and the Engineering Institute of Canada (FEIC). He is an Associate Editor (Features) of the *IEEE Antennas and Propagation Magazine* and served as Associate Editor of the IEEE TRANSACTIONS ON ANTENNAS AND PROPAGATION, *IEEE Antennas and Wireless Propagation*, and a member of the Editorial Board of the *RFMiCAE Journal*. In May 2002, he was awarded a Tier 1 Canada Research Chair position in Electromagnetic Engineering which has been renewed in 2009. In 2003, he received the 2003 Royal Military College "Excellence in Research" Prize. He was elected to the Board of the International Union of Radio Science (URSI) as Vice President in August 2008. He chaired conferences and has given plenary talks in many conferences, and supervised or co-supervised over 70 Ph.D. and M.Sc. theses at the Royal Military College and at Queen's University, of which several have received the Governor General of Canada Gold Medal as well as best paper awards in major symposia. He served as the Chairman of the Canadian National Commission for Radio Science (CNC, URSI, 1999–2008), Commission B National Chair (1993–1999), holds adjunct appointment at the University of Manitoba, and has a cross appointment at Queen's University in Kingston. He also serves, since November 2008, as Associate Director of the Defence and Security Research Institute (DSRI).